Fuel Processing Technology 265 (2024) 108150

Contents lists available at ScienceDirect

Fuel Processing Technology

journal homepage: www.elsevier.com/locate/fuproc

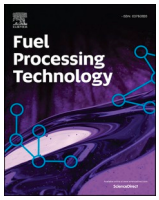

Catalytic steam reforming of waste tire pyrolysis volatiles using a tire char catalyst for high yield hydrogen-rich syngas

Yukun Li, Paul T. Williams *

School of Chemical and Process Engineering, University of Leeds, Leeds LS2 9JT, United Kingdom

ARTICLE INFO

Keywords:
Hydrogen/syngas
Pyrolysis
Catalysis
Steam gasification
Tire char

ABSTRACT

The production of hydrogen and syngas (H_2/CO) from waste tires by pyrolysis catalytic steam reforming was investigated in a two-stage fixed bed reactor. In this study, tire char served as a sacrificial catalyst, facilitating the combination of catalytic steam reforming and char steam gasification reactions. The tire char acted as both a catalyst and a gasification reactant, enhancing the gas product yield. The process parameters investigated were, a reforming temperature range of 700–1000 °C, steam space velocity between 2 and 12 g h^{-1} g_{char}^{-1} and reaction times of 0.5–2 h. The influence of the parameters on the yield and composition of the product gases and the characteristics of the used catalyst were analyzed in detail. The results indicated that higher temperature and steam space velocity increased H_2 and CO yields in the presence of a tire char catalyst. Elemental analysis of the used tire char, surface morphology and pore structure provided insights into the extent of tire char consumption in the reaction. Prolonged reaction time allowed for more thorough reactions between the pyrolysis volatiles and tire char, promoting the production of H_2. At a reaction time of 2 h, the H_2 yield reached 223 mmol g^{-1}, representing 74 wt% of the maximum hydrogen yield.

1. Introduction

With the rapid increase in global automobile production and usage, the large-scale generation of waste tires has become an undeniable environmental issue. It is estimated that about 3,000,000,000 tires are produced worldwide each year, these tires will eventually end up as waste tires which require management, treatment and disposal [1]. The options for the management of waste tires, include waste landfill, combustion in cement kilns, use in civil engineering applications and recycling to low quality products such as playground and sports surfaces [2]. However, there is interest in recovering the inherent resource of waste tires using pyrolysis technology which produces a char, oil and gas product [3–6]. The product distribution from the pyrolysis of tires is about 5 wt% gas, 58 wt% oil and 37 wt% char at 500 °C [3]. Pyrolysis gas is mainly composed of H_2, CO, CO_2 and CH_4, and has a high calorific value and can not only provide energy for the pyrolysis process itself but also can be used as fuel for gas turbines or internal combustion engines [7]. Tire pyrolysis oil is a high-energy-density liquid fuel that can be used as an alternative fuel for boilers or can be further refined into light oil products for use in vehicles or industrial equipment [5]. Gao et al. [1] have reviewed the various treatment options for tire pyrolysis char that have been investigated as routes to produce higher value products. Such options include, for example, the production of high surface area activated carbons through physical and chemical activation, the use of tire char as battery materials, recovery and use of carbon black and the use of tire char as a catalyst.

Due to the variable quality and high processing cost of pyrolysis oil, its market prospects are unclear. With the wide promotion of clean energy, the production and application of pyrolysis gas with clean energy properties will be expected to occupy a significant market share. To promote the clean and efficient use of energy, the research focus is gradually shifting to the production and optimization of high-quality pyrolysis gases. Some studies [8–11] have investigated the synergies between waste tires and biomass through co-pyrolysis to improve the quality of syngas. There have been reports on the further processing of the pyrolysis volatile oils and gases to produce hydrogen and syngas (H_2/CO) through catalytic steam reforming at catalyst temperatures of 700–900 °C [12–14]. For example, Elbaba et al. [13,14] used a two-stage pyrolysis-catalytic steam reforming process to produce a hydrogen-rich syngas from waste tires using nickel-based catalysts. Conventional metal catalysts such as Ni-based catalysts [15–17], Cu/zeolites [18,19], and Fe/Al_2O_3 [20,21] have been commonly used in

* Corresponding author.
E-mail address: p.t.williams@leeds.ac.uk (P.T. Williams).

https://doi.org/10.1016/j.fuproc.2024.108150
Received 4 September 2024; Received in revised form 24 October 2024; Accepted 28 October 2024
Available online 4 November 2024

pyrolysis catalytic steam reforming of waste tires. However, these catalysts were vulnerable to being deactivated by coke formation on the catalyst.

Some studies have proposed using pyrolysis char as a cost-effective and alternative catalyst. Research on the catalytic steam reforming of biomass pyrolysis volatiles has demonstrated that inherent alkali and alkaline earth metals in biochar exhibited tar-cracking activity, with additional metals further enhancing catalytic activity [22–26]. In addition, coal char was also used as a catalyst and catalyst support. Wang et al. [27] pointed out that coal char was an effective and inexpensive support for NiO to remove tar and purify syngas in biomass gasification. Given this, tire char has been explored as a catalyst in pyrolysis catalytic steam reforming of waste plastics and biomass [28–31]. Inorganic substances like Zn, Ca, Fe, and K present in tire char were important for syngas composition and tar cracking during the steam reforming process, as removing these metals resulted in a decrease in hydrogen yield under the same experimental conditions.

Using char as a sacrificial catalyst, whereby, the carbonaceous char becomes gasified during the steam reforming process has been proposed, in that the steam gasification of the char adds to the production of H_2 and CO [29,31]. For example, Al-Rahbi et al. [31] used a sacrificial tire char catalyst in the pyrolysis-catalytic steam reforming of biomass to increase the yield of hydrogen-rich syngas. Li et al. [29] also processed waste plastic pyrolysis volatiles using a tire char catalyst. Separate studies [32,33] on steam gasification of tire char have shown its potential for hydrogen production. For example, Lopez et al. [34], investigated the steam/oxygen gasification of granulated scrap tire char at 1000 °C and reported the hydrogen yield in the gasification products of different tire chars could reach 32–38 mmol g^{-1}. Therefore, simultaneous catalytic reforming and steam gasification could significantly enhance gas yield. A further negative issue for the use of tire char as a catalyst is that tires contain a small amount of sulfur, which is used in tire manufacture and during the pyrolysis process, this sulfur can be released in the form of H_2S, SOx [35]. These sulfides react with the catalyst metal to form metal sulfides, resulting in catalyst sulfur poisoning [36]. Xie et al. [37], pointed out that during steam reforming of liquid hydrocarbons, the presence of sulfur inducted more serious carbon deposition on the Ni catalyst surface. The role of sulfur in this work was not investigated, but is a topic for future work, since both tire pyrolysis and tire char gasification will release sulfur species into the product gas.

While the use of metal catalysts in catalytic steam reforming of waste tires has shown promise for syngas production, and significant progress has been made in studying the steam gasification of tire char, the use of tire char as a catalyst in catalytic pyrolysis of waste tires remains unexplored. In addition, the effects of reforming temperature, steam space velocity and reaction time on the production of H_2-rich syngas from waste tires processing in a two-stage reactor have not been systematically investigated. Hence, introducing catalytic gasification (using char with catalytic properties as a catalyst) into pyrolysis catalytic steam reforming of waste tires is proposed.

In this study, the effect of process parameters on product yield and properties was studied to optimize the reforming process and maximize the utilization of waste tire resources. Tire char derived from the pyrolysis of tires at 800 °C under a nitrogen atmosphere was used. Tire char steam gasification and pyrolysis catalytic steam reforming of waste tires were conducted at a range of temperatures (700, 800, 900 and 1000 °C), steam space velocities (2, 4, 6, 8, 10 and 12 g h^{-1} g_{char}^{-1}) and residence times (0.5,1 and 2 h). The reactivity between steam and tire char was assessed, and the effects of process parameters on gas yield, gas composition and the characteristics of the char catalyst were investigated.

2. Materials and methods

2.1. Materials

Waste truck tires were processed into ~5 mm particles by removing the steel components and then shredding and sieving. Multiple pyrolysis experiments (at 800 °C under a N_2 atmosphere) were conducted to produce sufficient tire char for subsequent experiments. The results indicated that the average yield of tire char was 36.50 wt%, pyrolysis oil was 55.50 wt%, and the yield of pyrolysis gas was 7.70 wt%, with a low standard relative deviation, demonstrating excellent repeatability.

The ultimate analysis and proximate analysis of the feedstock tire and produced tire char are shown in Table 1. Tires contain a high number of volatiles, which are released in an inert atmosphere under high-temperature conditions and converted into gases and liquids, thereby reducing the volatiles in the tire char. However, certain substances were difficult to decompose fully, resulting in residual high molecular weight volatiles in the tire char of 4.89 wt%. During the pyrolysis process, the mass of ash remained constant, with an increase in concentration occurring as a consequence of the volatile mass loss.

2.2. Experimental setup and procedure

The pyrolysis catalytic steam reforming of waste tire utilizing the derived tire char as the catalyst was conducted in a two-stage fixed-bed reactor (constructed of stainless steel). The two-stage reactors were externally heated by a controlled 1.5 kW electrical furnace. A schematic of the experimental setup is provided in Fig. 1. The reaction system consisted of a gas supply unit, a pyrolysis reactor, three-stage condensers, and a gas collection and analysis unit. The gas supply unit provided nitrogen and steam to the reactor. To ensure the proper position of the tire char within the catalytic reactor, a porous mesh was positioned centrally in the catalytic reactor, with quartz wool placed on top of the mesh to support the tire char catalyst. A continuous nitrogen flow rate of 100 ml min^{-1} was maintained to purge the product gases through the reactor and condenser system. Once the desired temperature (700 °C, 800 °C, 900 °C or 1000 °C) of second stage was reached and stabilized, the tire feedstock in the first stage pyrolysis reactor was heated from room temperature to 600 °C at a heating rate of 20 °C min^{-1}. The volatile products from pyrolysis were consequently passed into the catalytic steam reforming reactor for the reforming of the evolved mixture of hydrocarbon volatiles. Validation of the experimental reactor system demonstrated excellent repeatability over several repeat experiments, resulting in a standard deviation for the yields of gas of 1.34 wt%, for liquid of 0.93 wt% and for char of 0.02 wt%. The mass balance closure was ~100 wt% with a standard deviation of 1.19 wt%. For the char steam gasification, only the second stage (Fig. 1) was used as the gasification reactor, while the first stage pyrolysis reactor was kept empty. The experimental conditions were kept the same as the pyrolysis catalytic steam reforming process. The experimental design and conditions in this study are listed in Table 2.

2.3. Product analysis and characterization

Off-line gas chromatography (GC) (Varian CP-8380 instruments) was used to analyze the gas products. The hydrocarbons were carried by nitrogen purge gas into the column to be separated and detected by a flame ionization detector (FID), while permanent gases were carried by argon and detected by a thermal conductivity detector (TCD). Each gas was analyzed in triplicate, and the relative standard deviation was minimal, indicating an excellent repeatability. The gas yield was calculated based on molar percentage content using following equations:

$$V_{total\ gas} = \frac{F_{N_2} \times T}{C_{N_2}} \quad (1)$$

Table 1
Ultimate analysis and proximate analysis of tire and tire char.

Sample	Proximate analysis (wt%)				Ultimate analysis (wt%)				
	Moisture	Volatiles	Fixed carbon	Ash	C	H	N	S	O
Tire	0.95	66.99	27.61	4.62	78.35	7.08	0.44	2.54	5.63
Tire char	0.70	4.89	79.76	14.72	79.02	0.66	0.29	3.46	5.57

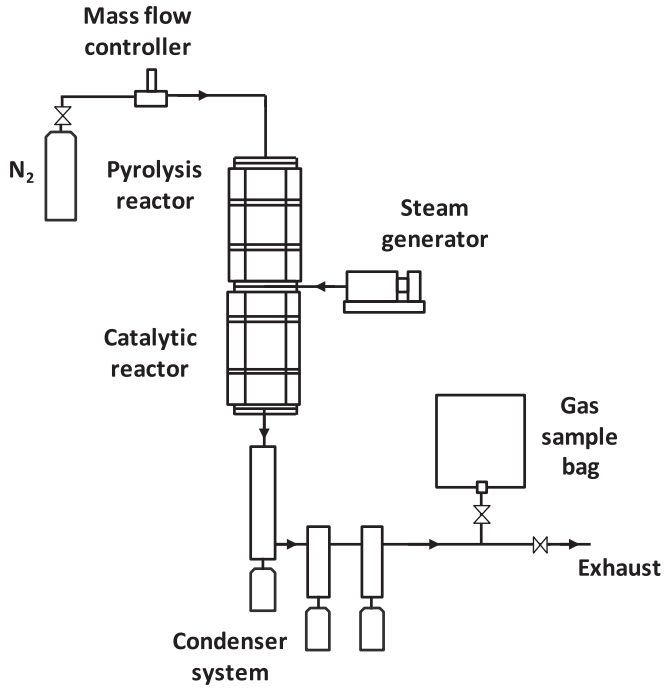

Fig. 1. Schematic diagram of the experimental system.

Table 2
Experimental design and conditions.

Char steam gasification			
	Gasification temperature (°C)	Steam space velocity (g h^{-1} g_{char}^{-1})	Reaction time (h)
Effect of gasification temperature	700, 800, 900, 1000	10	1
Effect of steam space velocity	1000	2, 4, 6, 8, 10, 12	1
Effect of reaction time	1000	10	0.5, 1, 2

Pyrolysis catalytic steam reforming				
	Pyrolysis temperature (°C)	Reforming temperature (°C)	Steam space velocity (g h^{-1} g_{char}^{-1})	Reaction time (h)
Effect of reforming temperature	600	700, 800, 900, 1000	10	1
Effect of steam space velocity	600	1000	2, 4, 6, 8, 10, 12	1
Effect of reaction time	600	1000	10	0.5, 1, 2

$$V_{gas} = V_{total\ gas} \times C_{gas} \tag{2}$$

$$Y_{gas}\left(mmol\ g_{tire}^{-1}\right) = \frac{V_{gas} \times M_{gas}}{22.4 \times M_{tire}} \tag{3}$$

$$Y_{gas}\left(mmol\ g_{char}^{-1}\right) = \frac{V_{gas} \times M_{gas}}{22.4 \times M_{char}} \tag{4}$$

where $V_{total\ gas}$ is the total gas collected, F_{N_2} is the nitrogen flowrate, T is the gas collection time, C_{N_2} is the nitrogen concentration, V_{gas} is the volume of each gas, C_{gas} is the concentration of each gas, M_{gas} is the mole of each gas, M_{tire} is the tire mass, M_{char} is the tire char mass. Eq. (3) was used to calculate the gas yield based on the tire only in the pyrolysis catalytic steam reforming of waste tire, and Eq. (4) was used to calculate the gas yield from tire char steam gasification.

The efficiency of the steam reforming process was evaluated by comparing experimental H_2 yield to theoretical H_2 yield, calculated by Eq. (5). Based on the theoretical H_2 yield concept in the pyrolysis catalytic process proposed by Czernik and French [38], the theoretical H_2 yield from the tire and tire char were calculated as 162.46 mmol g^{-1} and 136.12 mmol g^{-1}, respectively.

$$H_2\ potential\ (\%) = \frac{Experimental\ H_2\ yield}{Theoretical\ H_2\ yield} \tag{5}$$

Carbon conversion represents the release of carbon from the tire char, and the formula is as follows:

$$C\ conversion = \frac{mass\ of\ C\ in\ tire\ char - mass\ of\ C\ in\ tire\ char}{mass\ of\ C\ in\ tire\ char} \tag{6}$$

The ultimate analysis of feedstocks, fresh and used char materials was conducted using a Flash EA2000 elemental analyzer. The proximate analysis was carried out with a Mettler Toledo thermogravimetric analyzer (TGA). Inorganic elements in tire and tire char were analyzed with a Varian Fast Sequential Atomic Absorption Spectrophotometer (AAS). The porosity of char catalysts was examined by a Micrometrics Tristar 3000 instrument, with surface area calculated from nitrogen adsorption-desorption isotherms based on the Brunauer-Emmet-Teller (BET) method. The surface morphology and structure of char catalysts were characterized using a Hitachi SU8230 scanning electron microscope (SEM) at magnifications of 5000× and 30,000×. In addition, initial experiments assessing the steam reactivity of the tire char involved a thermogravimetric analyzer (Netzsch STA 449, F3, Jupiter TGA) supplied with steam.

3. Results and discussion

It has been shown previously that the gas composition from pyrolysis consists of H_2, CO, CO_2, H_2S and hydrocarbons such as CH_4, C_2H_4, C_2H_6, C_3H_6, C_3H_8, C_4H_8 and C_4H_6 [3,39]. Tire pyrolysis oil composition is a complex mixture of aliphatic, single ring aromatic, polycyclic aromatic hydrocarbons and cyclohydrocarbons in addition to heteroatomic hydrocarbons such as oxygen, nitrogen and sulfur containing species. Williams [3] lists more than 100 identified hydrocarbon species detected in tire pyrolysis oils. This complex mixture of volatile oils and gas components will all enter the catalytic steam reforming reactor and be reformed to produce H_2 and CO.

The pyrolysis catalytic steam reforming process involves a series of complex and competing reactions [31,40,41], as summarized in Table 3.

Table 3
Main reactions in the pyrolysis catalytic steam reforming process.

Name of reaction	Reactions	Number
Tire decomposition	$Tire \rightarrow Char + Tar + Gaseous\ (H_2, CO, CO_2, CH_4, C_nH_m)$	R1
Methane reforming	$CH_4 + H_2O \rightarrow CO + 3H_2$	R2
Hydrocarbon reforming	$C_nH_m + nH_2O \rightarrow nCO + \left[n + \left(\frac{m}{2}\right)\right]H_2$	R3
	$C_nH_m + 2nH_2O \rightarrow nCO_2 + (2n + m)H_2$	R4
Char gasification	$C + H_2O \rightarrow CO + H_2$	R5
	$C + 2H_2O \rightarrow CO_2 + 2H_2$	R6
Water gas shift reaction	$CO + H_2O \rightarrow CO_2 + H_2$	R7
Boudouard reaction	$C + CO_2 \rightarrow 2CO$	R8
Reactions of metal compounds	$ZnS + H_2O \rightarrow ZnO + H_2S$	R9
	$ZnS + 3H_2O \rightarrow ZnO + SO_2 + 3H_2$	R10
	$ZnO + C \rightarrow CO + Zn$	R11
	$Fe_3O_4 + C \rightarrow 3FeO + CO$	R12
	$FeO + C \rightarrow Fe + CO$	R13

These reactions are influenced by experimental conditions (such as reforming temperature, steam space velocity, residence time, etc.), which affect the gas products. The effects of different parameters were analyzed in the following sections.

3.1. Inorganic element composition and steam reactivity of char catalysts

The inorganic elements in tire char were characterized using AAS and are shown in Fig. 2(a). The analysis reveals that tire char contains a significant amount of Zn, along with other metals such as Fe, Ca. These elements have been shown to act as active phases or promoters in the steam reforming and char steam gasification process. For example, in the catalytic steam reforming of biomass volatiles, the introduction of Zn into a Fe/Al_2O_3 catalyst was shown to enhance the hydrogen yield, as Zn has been recognized to be an effective metal promoter in improving the performance of Fe active sites [42].

The results in terms of the steam reactivity of the tire char catalysts at various temperatures are presented in Fig. 2. From Fig. 2(b), it can be observed that as the temperature increased from 800 °C to 1000 °C within the first 12 mins, the sample mass decreased by about 6 wt%. This reduction may be attributed to releasing residual higher molecular weight volatiles in the tire char at higher temperatures. Miguel et al. [43] also noted that while tire pyrolysis was complete at 500 °C, the carbon yield slightly decreased when the temperature was further raised to 1000 °C. Fig. 2(b) further illustrates that at 800 °C, the mass of the sample gradually decreased at a rate of 0.16 wt% min^{-1}. However, at 1000 °C, the sample mass decreased sharply with a decomposition rate of 8.33 wt% min^{-1}. This indicated that tire char and steam exhibit higher reactivity at higher temperatures, because higher temperatures provide steam molecules with more energy to collide and react with carbon solid surfaces. Preciado-Hernandez et al. [44] also found that tire char steam gasification between 750 °C and 1050 °C increasing carbon conversion and gas-solid reaction rates.

3.2. Effect of reforming temperature

3.2.1. Effect of reforming temperature on gas products

Large molecular compounds (such as long-chain hydrocarbons, oxygenated compounds, etc.) are subjected to cracking or reforming reactions to generate smaller molecules such as gases and light oils in the pyrolysis catalytic steam reforming process [40,45]. These reactions are heavily influenced by the catalyst temperature. Four different reforming temperatures (700 °C, 800 °C, 900 °C, and 1000 °C) were investigated to study the effect of reforming temperature on the reforming reaction and the properties of the products. The steam input was set at 10 g h^{-1} g_{char}^{-1}, and the reaction time was fixed at 1 h.

Fig. 3(a) shows the hydrogen yield from two processes: tire char steam gasification and catalytic steam reforming of waste tires pyrolysis volatiles, across different reforming temperatures. The term "tire contribution" refers to the proportion of the gas yield from the steam reforming of tire pyrolysis volatiles relative to the total gas yield. To examine the impact of steam gasification on the pyrolysis catalytic process, a separate experiment of tire char steam gasification was conducted. As shown in Fig. 3(a), hydrogen produced from both processes increased with temperature, reaching 100 and 151 mmol g^{-1} respectively at 1000 °C. This is because reactions (R2-R7) are endothermic, and the rise in temperature promotes these reactions, thereby increasing hydrogen production. Zhai et al. [46] have shown that the temperature increase provided sufficient energy for steam molecules to overcome the activation energy, facilitating their reaction with carbon and hydrocarbons. Moreover, at high temperatures, the steam diffusion rate increased, thereby boosting the reaction rate. To demonstrate the catalytic effect of metals in tire char, a separate experiment was conducted using pure carbon with a similar specific surface area to that of the char catalyst in the second stage was conducted under the same experimental conditions. The hydrogen yield was 139 mmol g^{-1}, at a reforming temperature of 1000 °C which was lower than the hydrogen yield when tire char was used as the catalyst (151 mmol g^{-1}), indicating that the metals in the tire char promoted the steam reforming reaction and increased the hydrogen yield. The hydrogen yield contributed by waste tire pyrolysis volatiles also increased with reforming temperature, reaching 33.4 % of the total hydrogen yield at 1000 °C.

Fig. 3(b) shows the CO yield from tire char steam gasification and pyrolysis catalytic steam reforming experiments. At temperatures of 700 °C and 800 °C, tire char steam gasification was the dominant

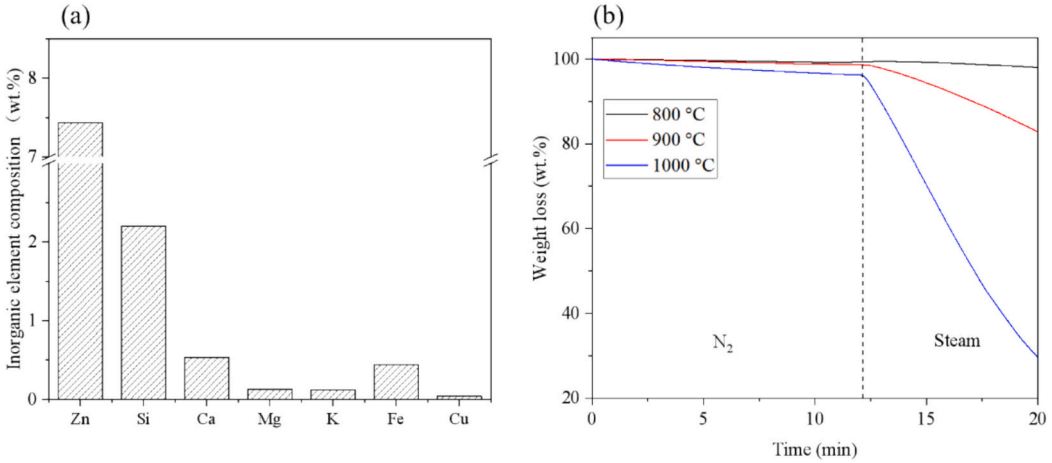

Fig. 2. (a) Inorganic element composition and (b) steam reactivity of tire char at different temperatures.

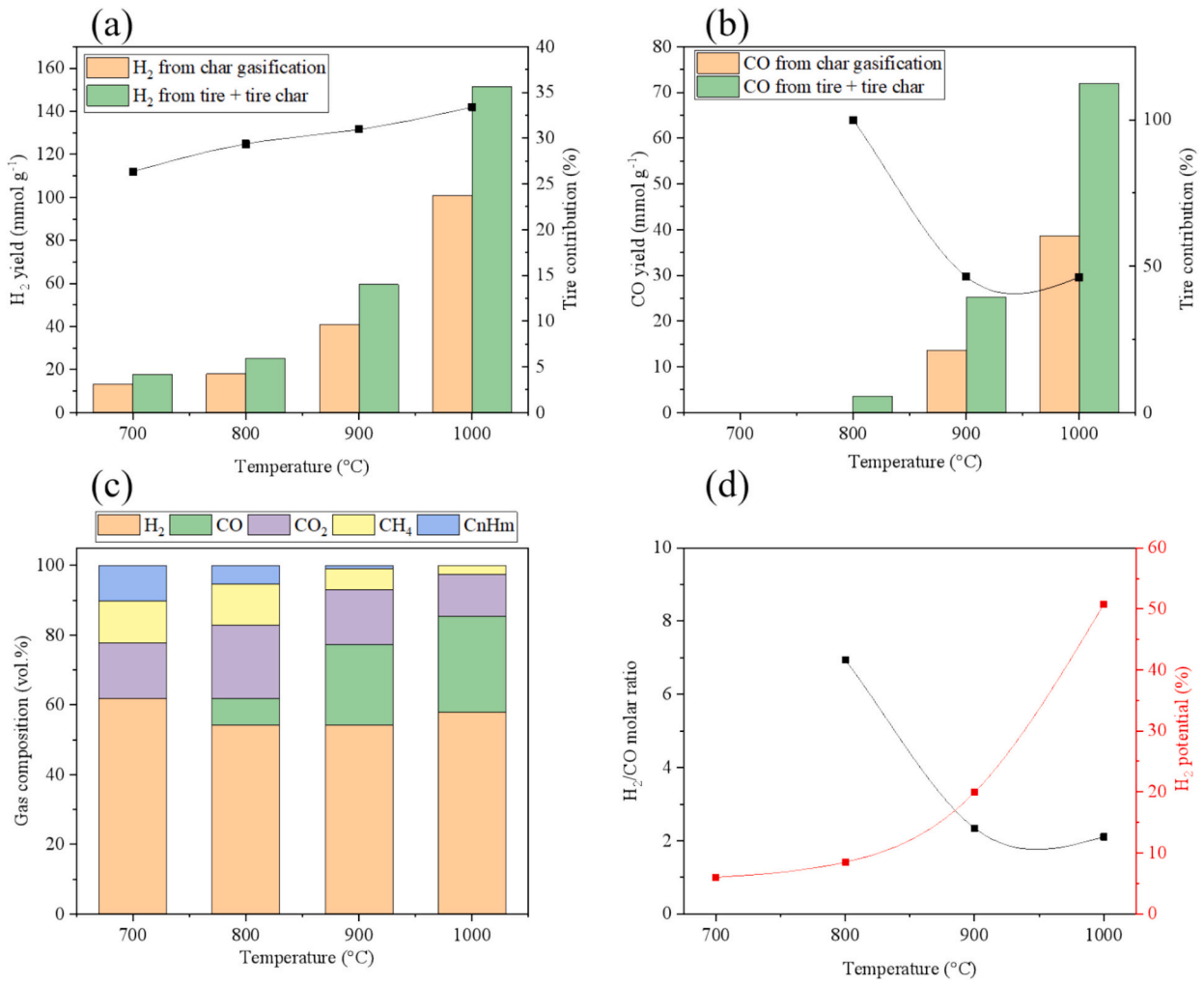

Fig. 3. Influence of reforming temperature on (a) H_2 yield, (b) CO yield, (c) gas composition and (d) H_2/CO molar ratio and H_2 potential.

process, and no CO was produced. However, at 800 °C, CO was detected in the pyrolysis catalytic process, possibly due to the steam reforming of tire pyrolysis volatiles (R2 and R3). At temperatures of 900 °C and 1000 °C, the CO yield from steam reforming of waste tires pyrolysis volatiles accounted for approximately 46.5 % of the total CO yield. Hu et al. [45] used activated carbon supported Fe/Ni catalyst to conduct pyrolysis catalytic experiments on pine wood, and they pointed out that the presence of the Boudouard reaction initiated CO_2 reduction and increased formation of CO at temperatures above 900 °C.

Fig. 3(c) shows the gas composition from both processes. When the temperature increased from 700 °C to 800 °C, the concentration of CO_2 increased from 16.1 % to 21 %. This rise was attributed to the tire char steam gasification (R6), which generated a significant amount of CO_2. As the temperature continued to rise, the Boudouard reaction (R8) became the dominant reaction, consuming the CO_2 produced and producing CO, which also explained the increase in CO concentration. Additionally, as the temperature rose from 700 to 1000 °C, the concentrations of CH_4 and CnHm decreased from 11.9 % to 2.5 % and 10.2 % to 0 %, respectively. Higher reforming temperature facilitated hydrocarbons reforming reactions (such as reactions R2-R4), and the resulting CO_2 was involved in the Boudouard reaction to produce CO with the sacrificial char catalyst. The H_2/CO molar ratio, crucial for syngas applications, is depicted in Fig. 3(d). At lower temperatures (700 °C and 800 °C), the minimal consumption of tire char resulted in a very high H_2/CO molar ratio. However, by 900 °C, the start of Boudouard reaction and a potential reduction in the water-gas shift reaction (R7) caused the H_2/CO molar ratio to drop sharply to approximately 2.3. Additionally, the intensification of the metal oxide reduction reaction (R11-R13) contributed to this decline. Hu et al. [45] pointed out that high temperatures facilitated the reaction between iron oxide and activated carbon support, thereby increasing the CO yield. Increasing the reforming temperature enhanced hydrogen potential, exceeding 50 % at 1000 °C. This suggested that high temperatures can more efficiently convert the hydrogen element in the feedstock into H_2.

3.2.2. *Effect of reforming temperature on char characteristics*

As a sacrificial catalyst, the tire char catalyst played dual roles in catalytic reforming. Firstly, its rich metal content facilitated the reforming of hydrocarbons. Secondly, it participated in char steam gasification and the Boudouard reaction as a reactant. Analyzing the transformation of char catalyst before and after the experiment can help to understand its function in the process. The changes of C and H elements, pore structure, and surface morphology of tire char recovered at different reforming temperatures were investigated.

Table 4 presents the C and H elements in tire char recovered at different reforming temperatures, along with carbon conversion and ash content. At 1000 °C, the ultimate analysis and BET surface area tests were not conducted because most of the tire char was consumed. The table shows that the content of carbon in tire char recovered was initially high but decreased as the reforming temperature was increased. Similarly, the content of hydrogen was low and also decreased with the increasing reforming temperature. This suggests that hydrogen in the

Table 4
Content of C, H elements, carbon conversion, and ash content of fresh and used tire char at different temperatures.

Sample	C (wt %)	H (wt %)	C conversion (%)	Char recovered (wt%)	Ash content (wt%)
Tire char	79.02	0.66			14.72
Tire char recovered at 700 °C	70.89	0.34	10.29	98	21.25
Tire char recovered at 800 °C	69.06	0.3	12.60	96	21.36
Tire char recovered at 900 °C	65.39	0.25	17.25	78	27.63

gas product was mainly generated from the reaction of carbon with steam and, to a lesser extent, from the hydrogen in the tire char [47]. At 700 °C, 10.29 wt% of the carbon was consumed, and as the temperature increased to 900 °C, more carbon was converted into gas. The rise in reforming temperature intensified the conversion of carbon into gas, consequently increasing the ash content, which heightened the probability of pyrolysis volatiles binding to the active sites. The study by Spiewak [32] also demonstrated a significant increase in carbon conversion when the temperature rose from 800 to 900 °C. During the steam reforming process, the ash content participated in the catalytic reactions and proved difficult to consume, so the increase in ash share in the tire char came at the expense of the carbon share.

To further explore the impact of reforming temperature on the pore structure of the char catalysts, the specific surface area, pore volume and pore diameter of char catalysts recovered at different reforming temperatures are summarized in Table 5. In our previous study [28], the specific surface area of tire char obtained after carbonization at 800 °C was 79 m^2/g. After steam reforming at 700 °C, the specific surface area exhibited negligible change, suggesting a low reactivity between tire char and steam at this temperature, which was also reflected in Fig. 2. However, with the reforming temperature increasing to 900 °C, the total specific surface area increased sixfold, reaching 497 m^2/g. Lopez et al. [33] also noted that higher temperatures enhanced the reactivity of carbon and steam, with the BET specific surface area of tire char after steam activated reaching ~500 $m^2\ g^{-1}$ at 900 °C. This phenomenon is mainly due to the accelerated diffusion rate of steam and gas products with rising temperatures, intensifying the carbon steam reaction. Consequently, a large amount of gas was released from the inside of the tire char, leading to the formation of cracks and increase in the specific surface area. In addition, CO_2 produced during the pyrolysis catalytic process contributes to developing pore structure. Molina-Sabio et al. [48] showed that CO_2 favored the formation of micropores during activation, while steam promoted the expansion of micropores. The increased specific surface area of micropores implied that more micropore structures were formed with increasing temperature, thus reducing the average pore diameter. Simultaneously, the total pore volume

Table 5
The pore properties of fresh and used tire char at different temperatures.

Sample	Surface area ($m^2\ g^{-1}$)	Micropore surface area ($m^2\ g^{-1}$)	Pore volume (cm^3/g)	Average pore size (nm)
Tire char	79.07	9.25	0.45	22.75
Tire char recovered at 700 °C	80.77	14.43	0.58	22.63
Tire char recovered at 800 °C	170.47	88.33	0.61	11.76
Tire char recovered at 900 °C	497.01	136.38	0.76	6.10

experienced an increase in temperature due to the generation of new pores and the expansion of existing ones. Zhang et al. [49] also pointed out that after tar reforming, the surface area and pore volume for all char catalysts increased to some extent. These changes in pore structure indicated that at high temperatures, the pore structure of the tire char catalyst would gradually become intricate, which increased the contact area for the pyrolysis volatiles and was conducive to the catalytic reaction.

The nitrogen adsorption and desorption isotherms, along with the pore size distributions of tire char recovered at different reforming temperatures, are shown in Fig. 4. As observed in Fig. 4(a), the adsorption and desorption isotherms of both tire char and tire char recovered at three temperatures all presented type IV curves [50], which is a characteristic of mesoporous materials. At low relative pressure ($P/P_0 < 0.1$), nitrogen adsorption increased rapidly, with tire char recovered at 900 °C showing significantly higher nitrogen adsorption than that at the other two temperatures, indicating a rich micropore structure, as reflected in the specific surface area of micropores (Table 5). Hysteresis loops occurred at moderate relative pressures. As the relative pressure approached 1, the nitrogen adsorption of all used tire char surged sharply, indicating the existence of mesopores (>20 nm) or macropores [51]. Fig. 4(b) illustrates the pore size distribution of both fresh and used tire char. It was evident that the pore size ranged between 2 and 100 nm, and the most prevalent size fell at 2–5 nm and 20–50 nm. This suggests that the pore size distribution experienced only slight changes after reforming reaction. Used tire char at 900 °C exhibited a notably more abundant pore structure in the 2–5 nm range compared to the other used tire chars, accompanied by a significant reduction in the average pore size, which was consistent with the results in Table 5. Zhang et al. [52] pointed out that the pore size of tire char after reacting with steam ranged from 0 to 102 nm, with a similar pore size distribution observed between 750 and 950 °C. However, a transition to larger pore sizes occurred with a continued rise in temperature to 1050 °C.

To further understand the evolution of the tire char surface morphology during the steam reforming process, SEM analysis was used. The corresponding images are shown in Fig. 5. In Fig. 5(a) the tire char surface at 5000× magnification reveals some raised granular structures. When the magnification was further increased to the nanometer scale (Fig. 5(b)), it became evident that these granular structures on the tire char surface were composed of spherical nanoparticles with relatively uniform size, and the size distribution of these nanoparticles was about 100–300 nm. In addition, the carbon steam reaction created surface defects in the tire char, resulting in the formation of noticeably larger pores. In comparison, the used tire char displayed a narrower particle size distribution and significantly smaller particle sizes, about 100 nm, indicating that the sample became more fully in contact with the pyrolysis volatiles during the reforming stage. As carbon reacted with steam, gases such as H_2, CO, and CO_2 were formed, which further affected the pore structure. This reaction likely contributed to the improved specific surface area and pore volume of the used tire char, as verified in the previous nitrogen adsorption-desorption experiment.

3.3. Effect of steam space velocity

3.3.1. Effect of steam space velocity on gas products

Fig. 6 presents the product yields and properties from tire char steam gasification and pyrolysis catalytic steam reforming experiments under varying steam space velocity. As shown in Fig. 6(a), increasing the steam input significantly enhanced the hydrogen yield from tire char steam gasification. As the steam input rose from 2 to 6 g h^{-1} g_{char}^{-1}, the H_2 yield experienced a rapid increase, rising from 26 to 80 mmol g^{-1}. Subsequently, with further increases in steam space velocity, the hydrogen yields gradually rose, eventually reaching 101 mmol g^{-1} at 10 g h^{-1} g_{char}^{-1}. However, beyond this point, the hydrogen yields stabilized. This is because steam was required in the initial reaction stages between carbon and steam. Zhai et al. [46] observed a similar trend in rice husk char

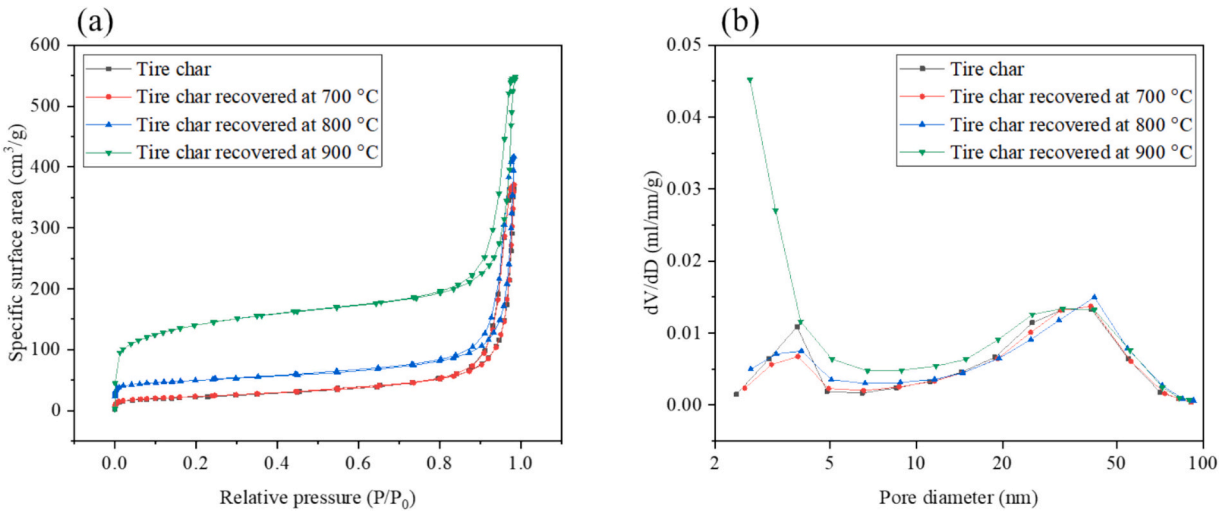

Fig. 4. (a) N_2 adsorption and desorption isotherm of fresh and used tire char and (b) pore size distribution at different temperatures.

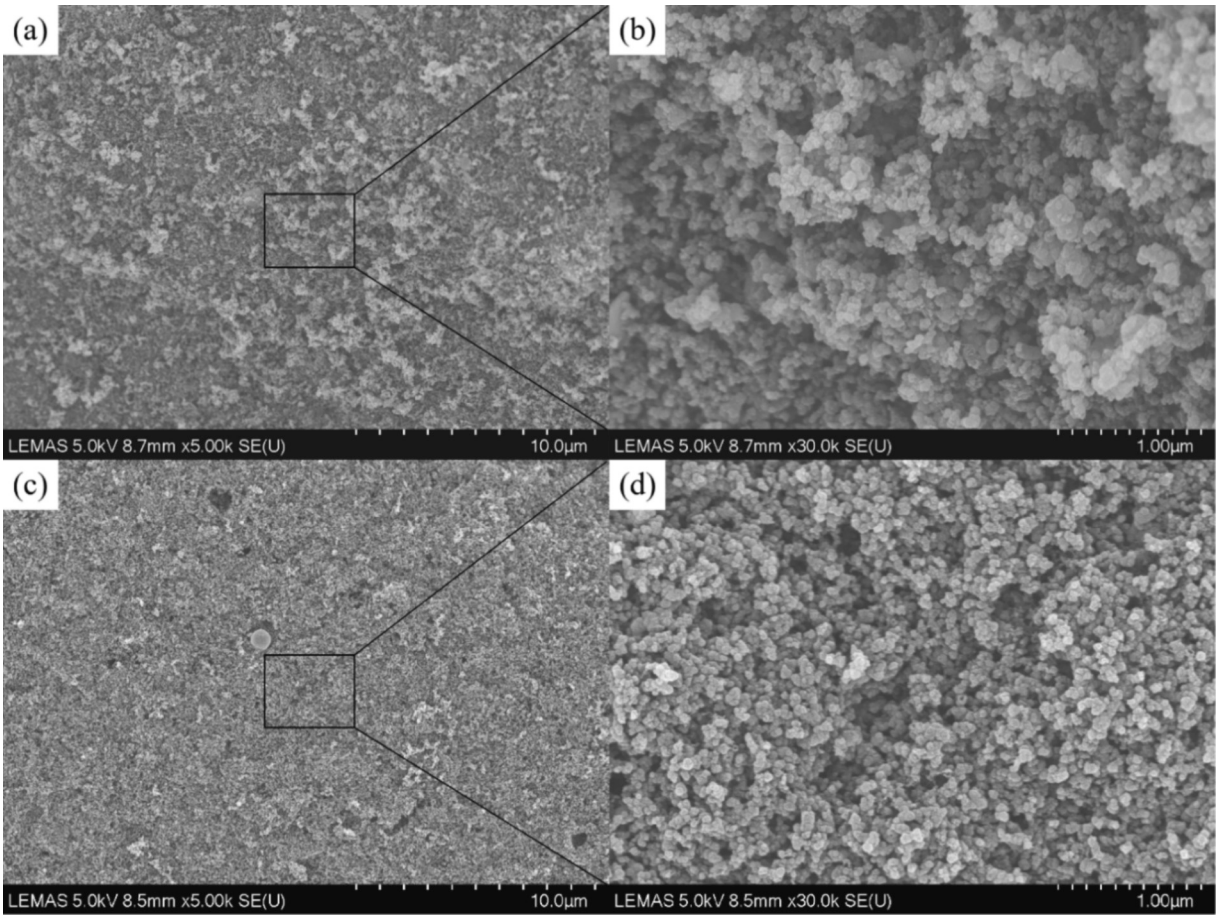

Fig. 5. SEM image of fresh and used tire char (a) tire char at a magnification of 5000, (b) tire char at a magnification of 30,000, (c) used tire char at 900 °C at a magnification of 5000 and (d) used tire char at 900 °C at a magnification of 30,000.

steam gasification, noting that excess steam beyond a certain point had little impact on carbon conversion and hydrogen generation. The hydrogen yield from the pyrolysis catalytic process followed a similar trend, with the hydrogen yield reaching about 152 mmol g^{-1} at 10 g h^{-1} g_{char}^{-1}. As the steam space velocity increased, the proportion of hydrogen contributed by tires rose rapidly before gradually declining, indicating that while increased steam space velocity can promote the steam reforming reactions, excessive steam had a minimal impact on further improving the reforming reaction.

As seen in Fig. 6(b), increasing the steam space velocity from 2 to 4 g h^{-1} g_{char}^{-1} led to a rapid initial increase in the CO yield from the tire char steam gasification, followed by a slower growth rate with further increase in steam. This phenomenon arises because at lower steam space velocity, char gasification (R5) required steam to convert into CO,

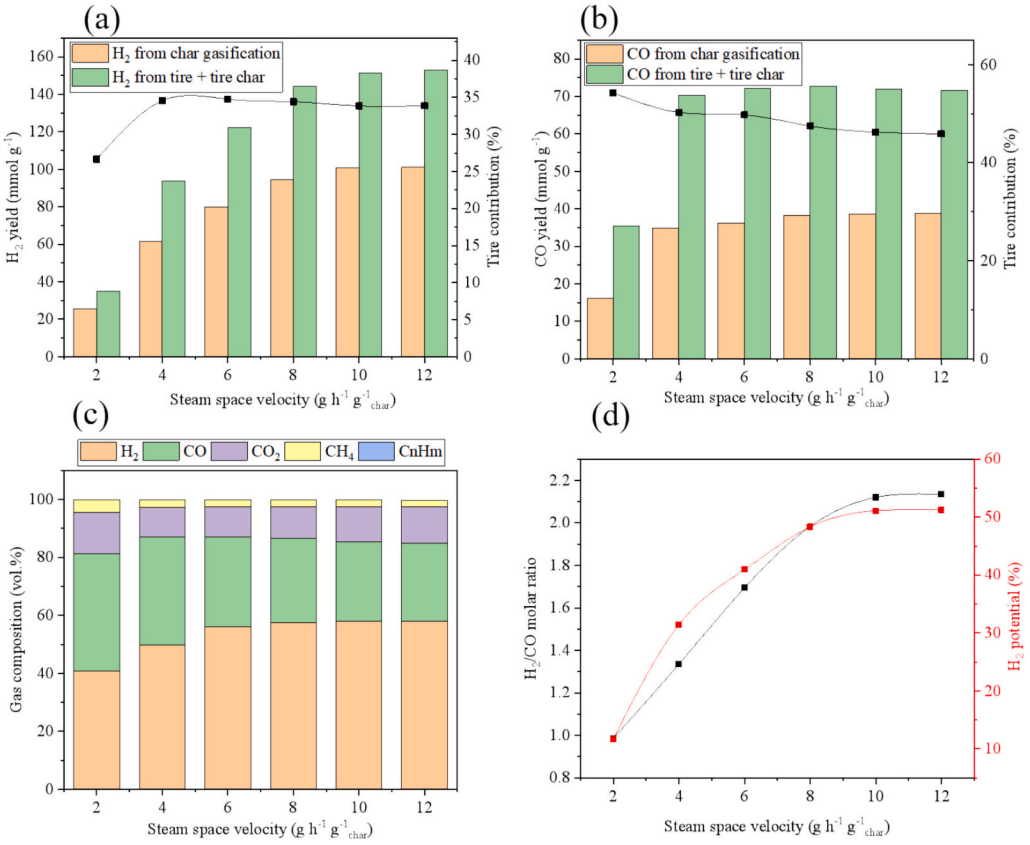

Fig. 6. Influence of steam space velocity on (a) H_2 yield, (b) CO yield, (c) gas composition and (d) H_2/CO molar ratio and H_2 potential.

whereas, at sufficient steam levels, the reaction (R5 and R7) reached equilibrium, stabilizing the formed CO. In the pyrolysis catalytic steam reforming experiment, when the steam input reached 8 g h^{-1} g_{char}^{-1}, the CO yield showed a slight downward trend, likely due to the promotion of reaction (R7). Furthermore, the proportion of CO contributed by tires gradually declined with increasing steam input, indicating the correlation between steam input and the catalytic impact of tire char catalyst.

At 1000 °C, the gas product from the pyrolysis catalytic experiment primarily comprised H_2, CO, and CO_2, and a small amount of CH_4. The gas composition under various steam input is shown in Fig. 6(c). As the steam space velocity increased from 2 to 12 g h^{-1} g_{char}^{-1}, the hydrogen concentration increased from 41 vol% to 58 vol%, while the CO concentration demonstrated a declining trend, decreasing from 40 vol% to 27 vol%. Moreover, with increasing steam space velocity, the total gas yield increased, whereas the CO yield remained relatively stable, resulting in a decrease in CO concentration. The CO_2 concentration exhibited a slight increase as the steam input was increased from 4 to 12 g h^{-1} g_{char}^{-1}, attributed to excessive steam space velocity promoting the water-gas shift reaction. Our previous study [53] on pyrolysis catalytic steam reforming of plastics using biochar as catalysts also showed that CO_2 concentration increased with the steam input increasing from 4 to 12 g h^{-1} g_{char}^{-1}. Additionally, the increase in steam space velocity led to a drop in CH_4 concentration from 4.5 vol% to approximately 2.5 vol%.

Fig. 6(d) shows the H_2/CO molar ratio and hydrogen potential from the pyrolysis catalytic steam reforming experiments at various steam space velocity. As the steam input was increased from 2 to 12 g h^{-1} g_{char}^{-1}, the H_2/CO molar ratio increased from 1 to approximately 2.13, indicating that steam can regulate the quality of the syngas. This is important, since different H_2/CO molar ratios are required for different end-use applications of the product syngas. For example, an ideal H_2/CO molar ratio for synthesis of liquid fuels is 1.7–2.2, aldehydes production via hydroformylation requires a H_2/CO ratio of 1:1 and for methanol production, a ratio between 1.5 and 2 is used. The increase in steam input promoted both H_2 and CO yields. The water-gas shift reaction was also promoted under the catalytic effect of tire char, thus increasing the H_2/CO molar ratio. Zhang et al. [54] showed that metallic elements in biochar (especially alkali and alkaline earth metals) can promote the absorption of steam on catalysts and the water gas shift reaction. Based on the ash composition of tire char, tire char contains Zn, Fe, Ca, Cu and other elements, which also have catalytic effects [29]. The hydrogen potential showed the same trend, with the hydrogen yield reaching 53 % of the total hydrogen yield at 12 g h^{-1} g_{char}^{-1}. The increased steam space velocity provided a large number of hydrogen radicals for the catalytic process, which freely combined with the hydrogen radicals generated by the dehydrogenation of hydrocarbons, thus producing more hydrogen.

3.3.2. *Effect of steam space velocity on char catalysts*

The change in C, H elements, carbon conversion, and ash content of the used tire char catalyst at various steam input is summarized in Table 6. At 6 g h^{-1} g_{char}^{-1}, about 40 wt% of the carbon reacted with the steam, resulting in the carbon content in the used tire char falling to 47.53 wt%. This phenomenon also explained the rapid increase in hydrogen production when the steam input ranged from 2 to 6 g h^{-1} g_{char}^{-1}. The H content also decreased with the rise of steam input, being

Table 6
The change of C, H elements, carbon conversion, and ash content of used tire char at various steam input.

Steam space velocity (g h^{-1} g_{char}^{-1})	C (wt %)	H (wt %)	C conversion (%)	Char recovered (wt%)	Ash content (wt%)
2	76.75	0.23	2.87	71	21.74
4	63.84	0.21	19.21	45	33.77
6	47.53	0.20	39.86	30	54.11

released in the form of gas. Meanwhile, the ash retained in the used tire char, leading to an increase in ash content.

The pore characteristics of used tire char under different steam input are shown in Table 7. As the steam input was increased from 2 to 4 g h^{-1} g_{char}^{-1}, the total specific surface area of used tire char increased from 506 m^2/g to 590 m^2/g. However, further increasing the steam input to 6 g h^{-1} g_{char}^{-1} resulted in a decrease in specific surface area to about 450 m^2/g. This is mainly because an optimal steam space velocity can lead to the formation of a rich pore structure in the tire char. Excessive steam, on the other hand, may cause the existing structure of the tire char to expand or even collapse, generating larger pores, and thereby reducing the specific surface area. Buentello-Montoya et al. [55] explored the effect of pore structure on the steam reforming of tar and noted that the specific surface area of catalysts rose while micropore areas decreased after steam reforming. The decrease in micropore specific surface area with increasing steam space velocity also indicated a reduction in micropore structure in tire char. Specifically, at 6 g h^{-1} g_{char}^{-1}, the specific surface area of the micropore was very small, measuring only 5.47 m^2/g. The pore volume of the used tire char showed a similar trend to the total specific surface area. A previous study [56] on the co-pyrolysis of coal and biomass for activated carbon production also showed that an excessive steam concentration reduced the total specific surface area of activated carbon while increasing the average pore diameter.

Fig. 7(a) shows the N_2 adsorption and desorption isotherms of fresh and used tire chars at different steam space velocity. The data shows that when the relative pressure was close to 0, the used tire char recovered at 2 g h^{-1} g_{char}^{-1} exhibited a rapid increase, surpassing the other two char. This suggested that the used tire char recovered at 2 g h^{-1} g_{char}^{-1} possessed a more abundant micropore structure. As the relative pressure increased, the nitrogen adsorption capacity of the tire char recovered at 4 g h^{-1} g_{char}^{-1} was the highest, followed by that at 6 g h^{-1} g_{char}^{-1}. This suggested that the macroporous structure of the tire char recovered at 4 g h^{-1} g_{char}^{-1} was more abundant than the other two chars. Fig. 7(b) illustrates the pore size distribution in the mesopores and micropores of the fresh and used tire char. It can be observed that the pores of both fresh and used tire char were mainly 2–5 and 20–50 nm in size range. With the increase of steam concentration, the tire char pores were more abundant, indicating that the steam concentration promotes the formation of pores. Zhang et al. [52] also pointed out that at 1050 °C, with the increase of the concentration of the activator (steam), the formation of the mesopore in tire char was enhanced.

Fig. 8 shows the SEM image of used tire char recovered at 1000 °C with different steam inputs. In Fig. 8(a), the surface of the tire char recovered at 2 g h^{-1} g_{char}^{-1} was relatively smooth, with some large pore structures. At 30,000 times magnification (Fig. 8(b)), it was evident that the sample contained numerous particles smaller than 100 nm, some of which were agglomerated to a certain extent due to interaction. In addition, a small number of large particles were exhibited, formed by the sintering of inorganic substances at high temperatures. The SEM image of tire char recovered at 6 g h^{-1} g_{char}^{-1} is shown in Fig. 8(c), exhibiting a rougher surface than that of tire char recovered at 2 g h^{-1} g_{char}^{-1}, and displaying rich and intricate structures. At a magnification of 30,000 (Fig. 8(d)), numerous very large particles were observed, and most of the nanoparticles were attached to these massive particles, forming agglomerations. Among these nanoparticles, carbon particles had a size of about 100 nm, while the very large particles had a particle size distribution range of about 1–2 μm. This indicated that at 6 g h^{-1} g_{char}^{-1}, steam reforming consumed more carbon and exposed the ash, significantly reducing the specific surface area of the sample. However, the consumption of carbon produced more syngas, and the exposure to ash facilitated the contact of volatiles with the active sites.

Table 7
The pore properties of the tire char recovered at different steam space velocity.

Steam space velocity (g h^{-1} $g_{catalyst}^{-1}$)	Total Surface area (m^2/g)	Micropore surface area (m^2/g)	Pore volume (cm^3/g)	Average pore size (nm)
2	506.81	184.80	0.82	6.47
4	589.66	67.94	0.91	6.19
6	448.55	5.47	0.85	7.62

3.4. Effect of char reaction time on-stream

The reaction time of the char catalyst on-stream is also an important parameter affecting the pyrolysis catalytic steam reforming process. As reaction time increased, pyrolysis oil volatiles and gases were adsorbed by the catalyst, allowing for more extended contact with steam and thus promoting the catalytic steam reforming reaction. The effects of three different reaction times (0.5 h, 1 h and 2 h) on the steam reforming process and gas products at 1000 °C and 10 g h^{-1} g_{char}^{-1} were studied, with the results shown in Fig. 9. Fig. 9(a) demonstrates that the hydrogen yield from tire char steam gasification initially experiences rapid growth followed by a slower increase, ultimately reaching 109 mmol g^{-1} at 2 h. This trend is due to the gradual consumption of tire char with prolonged steam gasification time, resulting in a decrease in the hydrogen generated by the reaction. In the pyrolysis catalytic steam reforming experiments, pyrolysis volatiles and tar from waste tires were initially adsorbed on the surface of catalysts and subsequently transformed into gas under the action of steam. Extended reaction time facilitated the conversion of these substances into gases. Wang et al. [57] prepared hydrogen-rich syngas by pyrolysis catalytic steam reforming of biomass using biochar as a catalyst and observed gas release at different times throughout the process. They noted that hydrogen yield peaked at 40 min, with another peak occurring at 70 min as the reaction progressed. Similarly, in this study, the hydrogen yield from tire pyrolysis volatiles increased as the reaction time extended from 1 h to 2 h. This indicated that the additional hydrogen produced during this time is mainly from the steam reforming of tar and hydrocarbons.

Fig. 9(b) illustrates the relationship between CO yield and residence time. After 1 h, the CO yield from tire char steam gasification and the pyrolysis catalytic process stabilized at about 39 mmol g^{-1} and 72 mmol g^{-1}, respectively. The reaction time of the tire char catalyst on stream minimally affects gas composition, with only a slight increase in the concentration of hydrogen and syngas. Prolonged reaction time ensured a more complete reaction between tire char and steam, increasing the hydrogen and syngas concentrations to 63 vol% and 86 vol%, respectively. The high concentrations of syngas in the gas products make them suitable for efficient utilization, as they can be readily purified through the adsorption or absorption of other gases (such as CO_2).

The H_2/CO molar ratio initially decreased and then increased over time, indicating that the Boudouard reaction was the predominant between 0.5 and 1 h. Beyond 1 h, most of the carbon in the tire char is consumed and converted into CO and CO_2, shifting the reaction dominance to the water gas shift reaction. The hydrogen potential increased from 22 % to 74 %, attributed to enhanced char gasification and steam reforming facilitated by extended residence time. Yan et al. [58] investigated the steam gasification of carbon generated from biomass, highlighting the significant role of prolonged solid reaction time in enhancing gas yield and carbon conversion efficiency. Similarly, Zhai et al. [46] investigated the effect of reaction time on the steam gasification of rice husk carbon, pointing out that longer reaction times facilitated a complete carbon-steam reaction and accelerate heat and mass transfer, thereby increasing conversion rates.

This study focused on enhancing hydrogen rich syngas by processing waste tires in a two-stage reactor using tire char as a catalyst. The tire char, rich in metal substances, effectively promoted both the steam reforming reactions of the hydrocarbons in the pyrolysis oil volatiles and gases (R2-R4) and the water gas shift reaction (R7). CH_4 was continuously dehydrogenated to form intermediates such as CH_3, CH_2, CH, and C in methane steam reforming (R2). Similarly, during the steam reforming of hydrocarbons, compounds represented as CnHm also

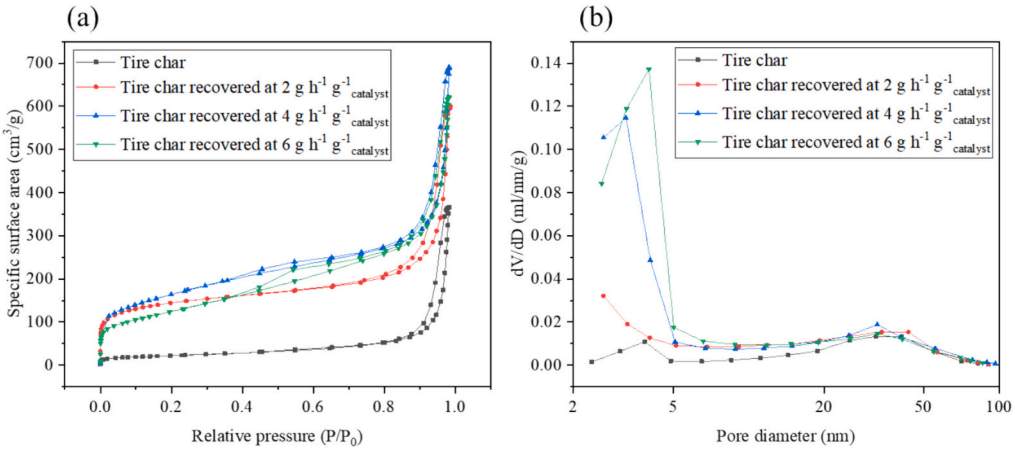

Fig. 7. (a) N_2 adsorption and desorption isotherms and (b) pore size distribution of the used tire chars in relation to different steam space velocity.

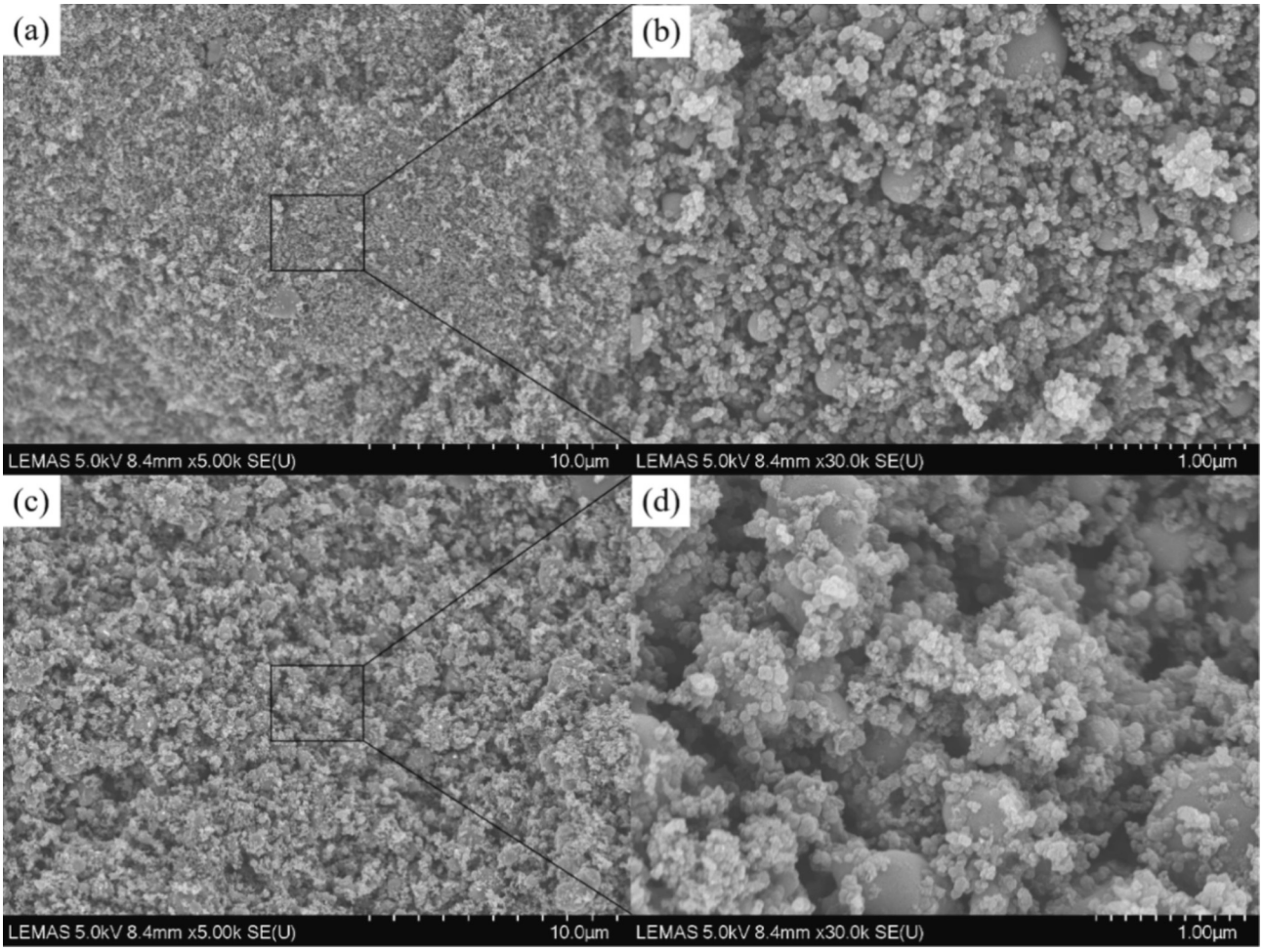

Fig. 8. SEM image of tire char recovered at 1000 °C. (a) tire char recovered at 2 g h^{-1} g^{-1}_{char} at a magnification of 5000, (b) tire char recovered at 2 g h^{-1} g^{-1}_{char} at a magnification of 30,000, (c) tire char recovered at 6 g h^{-1} g^{-1}_{char} at a magnification of 5000 and (d) tire char recovered at 6 g h^{-1} g^{-1}_{char} at a magnification of 30,000.

underwent continuous dehydrogenation to produce C and H. Steam decomposed into intermediates OH and H, and the O—H bonds in OH subsequently break to form H and O. These atoms then combined with C and H to form CO and H_2 [59,60]. In the water gas shift reaction (R7), CO and O combine to form CO_2. Wang et al. [59] demonstrated that metals catalysts reduced the activation energy barrier for methane and CnHm steam reforming reactions and promoted the production of hydrogen. In addition, compared to conventional catalysts, the carbon in tire char has a significant impact on the production of hydrogen and CO, via char gasification (R5, R6) and Boudouard reaction (R8) pathways. Introducing tire char effectively promotes the Boudouard reaction, converting CO_2 into CO, thereby boosting the yield of syngas. This work has also shown the influence of process parameters (reforming temperature, steam space velocity, residence time) on the catalytic process

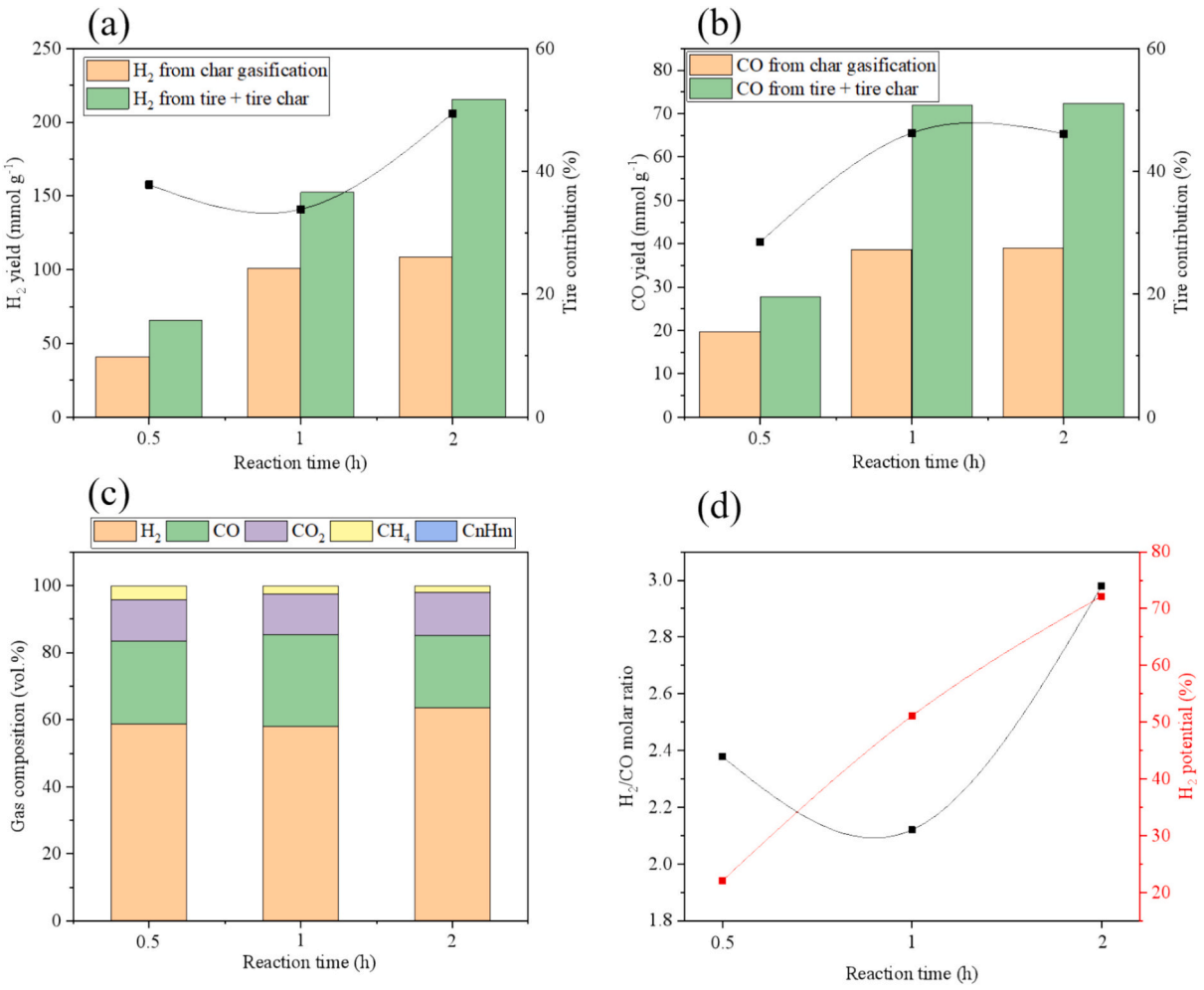

Fig. 9. Influence of reaction time on (a) H_2 yield, (b) CO yield, (c) gas composition and (d) H_2/CO molar ratio and H_2 potential.

and product properties were investigated under the interaction of tire char and steam. The process shows the potential of using a relatively low-cost char catalyst (byproducts obtained from waste tires) as a route to produce hydrogen-rich syngas. Based on the reactions and enthalpy changes involved in steam reforming and the combustion reaction of H_2 and CO, it is estimated that the heat generated by combustion is much greater than the heat absorbed during the steam reforming process, making the process economically worthwhile. Overall, this method of tire pyrolysis coupled with catalytic steam reforming offers a comprehensive approach to tire waste management, generating hydrogen-rich syngas from both oil volatiles and char, and using the hydrocarbon-rich pyrolysis gas as fuel to sustain the process.

4. Conclusions

H_2/CO syngas was produced by processing waste tires using tire char as a catalyst. The effects of various process parameters on gas products and char catalysts were investigated, and the conclusions are as follows.

(1) The reactivity between tire char and steam was improved with increasing temperature. At 1000 °C, the weight loss rate of tire char in the presence of steam reached 7.41 wt% min^{-1}.
(2) Both higher temperatures and steam space velocity intensified the reaction between the tire char and steam as well as the steam reforming of tire volatiles. This promoted the release of C and H elements, resulting in high H_2 and CO yields.
(3) Steam reacted with tire char, releasing gas and opening the pore structure of tire char. This process increased the specific surface area and micropore specific surface area, resulting in a more uniform particle distribution and smaller particle size of the char catalyst. However, excessive temperature and steam input could cause the collapse of pore structure, reducing the specific surface area.
(4) Extending the reaction time of the tire char effectively converted tire pyrolysis volatiles and carbon in tire char into gas. At 2 h, the H_2 yield reached 223 mmol g^{-1}, corresponding to 74 % of the maximum H_2 yield.
(5) As the reaction progresses, the specific surface area of the catalyst increases, making it less prone to deactivation during long-term experiments and providing more contact area for hydrocarbons. In future research, the effects of the catalyst pore structure and surface properties can be further studied.

CRediT authorship contribution statement

Yukun Li: Writing – original draft, Investigation. **Paul T. Williams:** Writing – review & editing, Supervision, Funding acquisition.

Declaration of competing interest

The authors declare that they have no known competing financial interests or personal relationships that could have appeared to influence the work reported in this paper.

Data availability

Data will be made available on request.

Acknowledgements

Yukun Li was awarded a China Scholarship Council - University of Leeds scholarship (202106220059) to carry out the research which is gratefully acknowledged.

References

[1] N. Gao, F. Wang, C. Quan, L. Santamaria, G. Lopez, P.T. Williams, Tire pyrolysis char: Processes, properties, upgrading and applications, Prog. Energy Combust. Sci. 93 (2022) 101022.
[2] M. Sienkiewicz, J. Kucinska-Lipka, H. Janik, A. Balas, Progress in used tyres management in the European Union: a review, Waste Manag. 32 (10) (2012) 1742–1751.
[3] P.T. Williams, Pyrolysis of waste tyres: a review, Waste Manag. 33 (8) (2013) 1714–1728.
[4] W. Han, D. Han, H. Chen, Pyrolysis of waste tires: a review, Polymers 15 (7) (2023) 1604.
[5] J.D. Martínez, N. Puy, R. Murillo, T. García, M.V. Navarro, A.M. Mastral, Waste Tyre pyrolysis–a review, Renew. Sust. Energ. Rev. 23 (2013) 179–213.
[6] A.A. Al-Qadri, U. Ahmed, N. Ahmad, A.G.A. Jameel, U. Zahid, S.R. Naqvi, A review of hydrogen generation through gasification and pyrolysis of waste plastic and tires: Opportunities and challenges, Int. J. Hydrog. Energy 77 (2024) 1185–1204.
[7] D. Czajczyńska, R. Krzyżyńska, H. Jouhara, N. Spencer, Use of pyrolytic gas from waste tire as a fuel: a review, Energy 134 (2017) 1121–1131.
[8] Z. Wang, K.G. Burra, T. Lei, A.K. Gupta, Co-gasification characteristics of waste tire and pine bark mixtures in CO2 atmosphere, Fuel 257 (2019) 116025.
[9] Z. Wang, K.G. Burra, M. Zhang, X. Li, M. Policella, T. Lei, A.K. Gupta, Co-pyrolysis of waste tire and pine bark for syngas and char production, Fuel 274 (2020) 117878.
[10] Z. Wang, S. Guo, G. Chen, M. Zhang, T. Sun, Y. Chen, M. Wu, X. Xin, S. Yang, T. Lei, Synergistic effects and kinetics in co-pyrolysis of waste tire with five agricultural residues using thermogravimetric analysis, J. Energ. Resour. Technol. 145 (12) (2023).
[11] Z. Wang, Y. Chen, G. Chen, T. Sun, M. Zhang, Q. Wang, M. Wu, S. Guo, S. Yang, T. Lei, Products distribution and Synergistic Effects Analysis during Co-Pyrolysis of Agricultural Residues and Waste Tire using Gas Chromatography/Mass Spectrometry, J. Energ. Resour. Technol. 145 (8) (2023) 081501.
[12] S. Portofino, A. Donatelli, P. Iovane, C. Innella, R. Civita, M. Martino, D.A. Matera, A. Russo, G. Cornacchia, S. Galvagno, Steam gasification of waste Tyre: Influence of process temperature on yield and product composition, Waste Manag. 33 (3) (2013) 672–678.
[13] I.F. Elbaba, P.T. Williams, Two stage pyrolysis-catalytic gasification of waste tyres: Influence of process parameters, Appl. Catal. B Environ. 125 (2012) 136–143.
[14] I.F. Elbaba, C. Wu, P.T. Williams, Catalytic pyrolysis-gasification of waste tire and tire elastomers for hydrogen production, Energy Fuel 24 (7) (2010) 3928–3935.
[15] Z. Li, Q. Yang, L. Tao, X. Ma, J. Zhou, T. Ye, J. Wu, R. Wu, H. Ben, Formation mechanism of hydrogen production from catalytic pyrolysis of waste tires: a ReaxFF molecular dynamics and experimental study, Fuel 341 (2023) 127664.
[16] Z. Li, L. Tao, Q. Yang, L. Chen, H. Qi, X. Ma, H. Ben, Mechanism research on hydrogen production from catalytic pyrolysis of waste tire rubber, Fuel 331 (2023) 125846.
[17] P. Osorio-Vargas, T. Menares, I.D. Lick, M.L. Casella, R. Romero, R. Jiménez, L. E. Arteaga-Pérez, Tuning the product distribution during the catalytic pyrolysis of waste tires: the effect of the nature of metals and the reaction temperature, Catal. Today 372 (2021) 164–174.
[18] Q. Cao, K. Xie, W. Bao, W. Huang, J. Zhao, Pyrolysis of waste tires with copper nitrate, Energy Sources 26 (4) (2004) 397–407.
[19] J. Yu, S. Liu, A. Cardoso, Y. Han, K. Bikane, L. Sun, Catalytic pyrolysis of rubbers and vulcanized rubbers using modified zeolites and mesoporous catalysts with Zn and Cu, Energy 188 (2019) 116117.
[20] Y. Zhang, C. Wu, M.A. Nahil, P. Williams, Pyrolysis–catalytic reforming/gasification of waste tires for production of carbon nanotubes and hydrogen, Energy Fuel 29 (5) (2015) 3328–3334.
[21] W. Li, M. Wei, Y. Liu, Y. Ye, S. Li, W. Yuan, M. Wang, D. Wang, Catalysts evaluation for production of hydrogen gas and carbon nanotubes from the pyrolysis-catalysis of waste tyres, Int. J. Hydrog. Energy 44 (36) (2019) 19563–19572.
[22] L. Wei, S. Xu, L. Zhang, C. Liu, H. Zhu, S. Liu, Steam gasification of biomass for hydrogen-rich gas in a free-fall reactor, Int. J. Hydrog. Energy 32 (1) (2007) 24–31.
[23] Z. Min, P. Yimsiri, M. Asadullah, S. Zhang, C. Li, Catalytic reforming of tar during gasification. Part II. Char as a catalyst or as a catalyst support for tar reforming, Fuel 90 (7) (2011) 2545–2552.
[24] D. Yao, Q. Hu, D. Wang, H. Yang, C. Wu, X. Wang, H. Chen, Hydrogen production from biomass gasification using biochar as a catalyst/support, Bioresour. Technol. 216 (2016) 159–164.
[25] L. Cheng, Z. Wu, Z. Zhang, C. Guo, N. Ellis, X. Bi, A.P. Watkinson, J.R. Grace, Tar elimination from biomass gasification syngas with bauxite residue derived catalysts and gasification char, Appl. Energy 258 (2020) 114088.
[26] S. Wang, R. Shan, T. Lu, Y. Zhang, H. Yuan, Y. Chen, Pyrolysis char derived from waste peat for catalytic reforming of tar model compound, Appl. Energy 263 (2020) 114565.
[27] D. Wang, W. Yuan, W. Ji, Char and char-supported nickel catalysts for secondary syngas cleanup and conditioning, Appl. Energy 88 (5) (2011) 1656–1663.
[28] Y. Li, M.A. Nahil, P.T. Williams, Pyrolysis-catalytic steam reforming of waste plastics for enhanced hydrogen/syngas yield using sacrificial tire pyrolysis char catalyst, Chem. Eng. J. 467 (2023) 143427.
[29] Y. Li, M.A. Nahil, P.T. Williams, Hydrogen/syngas production from different types of waste plastics using a sacrificial tire char catalyst via pyrolysis–catalytic steam reforming, Energy Fuel 37 (9) (2023) 6661–6673.
[30] J. Husár, J. Haydary, P. Šuhaj, P. Steltenpohl, Potential of tire pyrolysis char as tar-cracking catalyst in solid waste and biomass gasification, Chem. Pap. 73 (2019) 2091–2101.
[31] A.S. Al-Rahbi, P.T. Williams, Hydrogen-rich syngas production and tar removal from biomass gasification using sacrificial Tyre pyrolysis char, Appl. Energy 190 (2017) 501–509.
[32] K. Śpiewak, G. Czerski, P. Soprych, Steam gasification of tire char supported by catalysts based on biomass ashes, Energy 285 (2023) 129378.
[33] G. López, M. Olazar, M. Artetxe, M. Amutio, G. Elordi, J. Bilbao, Steam activation of pyrolytic Tyre char at different temperatures, J. Anal. Appl. Pyrolysis 85 (1–2) (2009) 539–543.
[34] F.A. López, T.A. Centeno, F.J. Alguacil, B. Lobato, A. López-Delgado, J. Fermoso, Gasification of the char derived from distillation of granulated scrap tyres, Waste Manag. 32 (4) (2012) 743–752.
[35] S. Kordoghli, B. Khiari, M. Paraschiv, F. Zagrouba, M. Tazerout, Production of hydrogen and hydrogen-rich syngas during thermal catalytic supported cracking of waste tyres in a bench-scale fixed bed reactor, Int. J. Hydrog. Energy 44 (22) (2019) 11289–11302.
[36] Y. Chen, C. Xie, Y. Li, C. Song, T.B. Bolin, Sulfur poisoning mechanism of steam reforming catalysts: an X-ray absorption near edge structure (XANES) spectroscopic study, Phys. Chem. Chem. Phys. 12 (21) (2010) 5707–5711.
[37] C. Xie, Y. Chen, Y. Li, X. Wang, C. Song, Sulfur poisoning of CeO2–Al2O3-supported mono-and bi-metallic Ni and Rh catalysts in steam reforming of liquid hydrocarbons at low and high temperatures, Appl. Catal. A Gen. 390 (1–2) (2010) 210–218.
[38] S. Czernik, R.J. French, Production of hydrogen from plastics by pyrolysis and catalytic steam reform, Energy Fuel 20 (2) (2006) 754–758.
[39] D. Leung, X. Yin, Z. Zhao, B. Xu, Y. Chen, Pyrolysis of tire powder: influence of operation variables on the composition and yields of gaseous product, Fuel Process. Technol. 79 (2) (2002) 141–155.
[40] F. Guo, X. Li, Y. Liu, K. Peng, C. Guo, Z. Rao, Catalytic cracking of biomass pyrolysis tar over char-supported catalysts, Energy Convers. Manag. 167 (2018) 81–90.
[41] M. Hatori, E. Sasaoka, M.A. Uddin, Role of TiO_2 on oxidative regeneration of spent high-temperature desulfurization sorbent ZnO-TiO_2, Ind. Eng. Chem. Res. 40 (8) (2001) 1884–1890.
[42] F. Chen, C. Wu, L. Dong, F. Jin, P.T. Williams, J. Huang, Catalytic steam reforming of volatiles released via pyrolysis of wood sawdust for hydrogen-rich gas production on Fe–Zn/Al_2O_3 nanocatalysts, Fuel 158 (2015) 999–1005.
[43] G.S. Miguel, G.D. Fowler, C.J. Sollars, Pyrolysis of tire rubber: porosity and adsorption characteristics of the pyrolytic chars, Ind. Eng. Chem. Res. 37 (6) (1998) 2430–2435.
[44] J. Preciado-Hernandez, J. Zhang, I. Jones, M. Zhu, Z. Zhang, D. Zhang, An experimental study of gasification kinetics during steam activation of a spent Tyre pyrolysis char, J. Environ. Chem. Eng. 9 (4) (2021) 105306.
[45] J. Hu, Z. Jia, S. Zhao, W. Wang, Q. Zhang, R. Liu, Z. Huang, Activated char supported Fe-Ni catalyst for syngas production from catalytic gasification of pine wood, Bioresour. Technol. 340 (2021) 125600.
[46] M. Zhai, Y. Zhang, P. Dong, P. Liu, Characteristics of rice husk char gasification with steam, Fuel 158 (2015) 42–49.
[47] Z. Cheng, M. Li, J. Li, F. Lin, W. Ma, B. Yan, G. Chen, Transformation of nitrogen, sulfur and chlorine during waste tire pyrolysis, J. Anal. Appl. Pyrolysis 153 (2021) 104987.
[48] M. Molina-Sabio, M. Gonzalez, F. Rodriguez-Reinoso, A. Sepúlveda-Escribano, Effect of steam and carbon dioxide activation in the micropore size distribution of activated carbon, Carbon 34 (4) (1996) 505–509.
[49] S. Zhang, M. Asadullah, L. Dong, H. Tay, C. Li, An advanced biomass gasification technology with integrated catalytic hot gas cleaning. Part II: Tar reforming using char as a catalyst or as a catalyst support, Fuel 112 (2013) 646–653.
[50] M.D. Donohue, G.L. Aranovich, Classification of Gibbs adsorption isotherms, Adv. Colloid Interf. Sci. 76 (1998) 137–152.
[51] T. Zhu, J. Zhou, Z. Li, S. Li, W. Si, S. Zhuo, Hierarchical porous and N-doped carbon nanotubes derived from polyaniline for electrode materials in supercapacitors, J. Mater. Chem. A 2 (31) (2014) 12545–12551.
[52] J. Zhang, I. Jones, M. Zhu, Z. Zhang, J. Preciado-Hernandez, D. Zhang, Pore development during CO_2 and steam activation of a spent Tyre pyrolysis char, Waste Biomass Valoriz. 12 (2021) 2097–2108.
[53] Y. Li, P.T. Williams, Catalytic Biochar and Refuse-Derived Char for the Steam Reforming of Waste Plastics Pyrolysis Volatiles for Hydrogen-Rich Syngas, Ind. Eng. Chem. Res. 62 (36) (2023) 14335–14348.
[54] S. Zhang, Z. Chen, Q. Cai, D. Ding, The integrated process for hydrogen production from biomass: Study on the catalytic conversion behavior of pyrolytic vapor in gas–solid simultaneous gasification process, Int. J. Hydrog. Energy 41 (16) (2016) 6653–6661.

[55] D. Buentello-Montoya, X. Zhang, J. Li, V. Ranade, S. Marques, M. Geron, Performance of biochar as a catalyst for tar steam reforming: effect of the porous structure, Appl. Energy 259 (2020) 114176.
[56] Y. Li, L. Lu, S. Lyu, H. Xu, X. Ren, Y.A. Levendis, Activated coke preparation by physical activation of coal and biomass co-carbonized chars, J. Anal. Appl. Pyrolysis 156 (2021) 105137.
[57] Y. Wang, L. Huang, T. Zhang, Q. Wang, Hydrogen-rich syngas production from biomass pyrolysis and catalytic reforming using biochar-based catalysts, Fuel 313 (2022) 123006.
[58] F. Yan, S. Luo, Z. Hu, B. Xiao, G. Cheng, Hydrogen-rich gas production by steam gasification of char from biomass fast pyrolysis in a fixed-bed reactor: Influence of temperature and steam on hydrogen yield and syngas composition, Bioresour. Technol. 101 (14) (2010) 5633–5637.
[59] J. Wang, B. Zhao, S. Liu, D. Zhu, F. Huang, H. Yang, H. Guan, A. Song, D. Xu, L. Sun, Catalytic pyrolysis of biomass with Ni/Fe-CaO-based catalysts for hydrogen-rich gas: DFT and experimental study, Energy Convers. Manag. 254 (2022) 115246.
[60] J. Song, Y. Pan, J. Wang, J. Wang, A. Cao, A. Wu, P.T. Williams, Q. Huang, Low-temperature hydrogen production from waste polyethylene by nonthermal plasma (NTP)-assisted catalytic pyrolysis using NiCeOx/β catalyst, Chem. Eng. J. 490 (2024) 151676.